

System Design and Assessment Notes

Note 37

Susceptibility of Some Electronic Equipment to HPEM Threats

28 February 2004

Michael Camp², Daniel Nitsch¹, Frank Sabath¹,
Jan-Luiken ter Haseborg³, Heyno Garbe²

¹ GAF Institute for Protective Technologies, Munster, Germany

² University of Hannover, Germany

³ Technical University of Hamburg Harburg

Abstract

In this note an overview of the susceptibility of a large number of different electronic devices like Computer Networks, Computer Systems, Microprocessor Boards, Microcontrollers and other basic integrated circuits (ICs) to different threats like EMP, UWB and HPM is given. The presented data will include a comparison of the HPM and UWB susceptibility of some devices and a deeper look into the destruction effects in ICs. Therefore the ICs were opened and the destruction effects were investigated. A norm based approach to describe the threat of different pulses to electronic devices gives a theoretical explanation for the measured susceptibility data.

I. INTRODUCTION

Communication, data processing, sensors and similar electronic devices are vital parts of the modern technical environment. Damage or failures in those devices could lead to technical or financial disasters as well as injuries or the loss of life. The significant progress of the HPEM source and antenna technologies and the easy access to simple HPEM systems entail the need to determine the susceptibility of electronic equipment to those threats.

The assessment of different circuit and pulse parameters on the upset and destruction effects are important to develop models for the susceptibility behavior and protection elements.

II. THREAT PARAMETERS

In our investigations three different HPEM pulse threats were applied to the equipment under test (EUT): Double Exponential Pulses, Bipolar Pulses and Microwave Pulses.

Nuclear Electromagnetic Pulses (NEMP) and unipolar Ultra Wide Band Pulses (UWB) generally have a double exponential pulse shape with the characteristic parameters rise time (t_r), the maximum electric field strength (E_{max}) and the full width half max time (t_{fwhm}). Radiated pulses usually have a bipolar pulse shape which is characterized by the rise and fall time (t_r and t_f) the time between maximum and minimum field strength (t_{pp}) and the maximum electric field strength (E_{max}). High Power Microwave Pulses (HPM) are characterized by the maximum electric field strength (E_{max}), their duration (t_d) and their center frequency (f_c). Table I shows some typical parameters for the different HPEM threats.

TABLE I
TYPICAL PARAMETERS FOR NEMP, UWB, HPM

Pulse Shape	Parameter 1	Parameter 2	Parameter 3
NEMP	t_r few ns	t_{fwhm} 20 – 400 ns	E_{max} 50 kV/m
Unipolar UWB	t_r 90 – 250 ps	t_{fwhm} few ns	E_{max} 1 – 100 kV/m ¹
Bipolar UWB	t_r/t_f 50 – 250 ps	t_{pp} 100 – 500 ps	E_{max} 1 – 100 kV/m ¹
HPM	f_c 500 MHz – 5 GHz	t_d 50 – 500 ns	E_{max} 1 – 100 kV/m ¹

¹Field Strength is depending on the distance between the source and the target
Peak value of the electrical field

III. DEFINITIONS

To describe the different failure effects two quantities were defined. The Breakdown Failure Rate (*BFR*) was defined as the number of breakdowns of a system, divided by the number of pulses applied to it (see Figure 1). A breakdown means no physical damage is done to the system. After a reset (self-, external- or power reset) the system is going back into function. The Breakdown Threshold (BT) specifies the value of the electrical field strength, at which the BFR gets 5% of the maximum value.

The Breakdown Bandwidth (BB) is defined as the span of the electrical field strength, in which the BFR changes from 5% to 95% of the maximum. The Destruction Failure Rate (DFR) of the device under test has been defined as the number of destructions divided by the number of pulses applied to the system. Destruction is defined as a physical damage of the system so that the system will not recover without a hardware repair.

$$\|V(j\omega)\|_{f,p}^{(f_1,f_2)} = \left\{ \int_{f_1}^{f_2} |V(j\omega)|^p d\omega \right\}^{\frac{1}{p}} \quad (1)$$

As shown in [1] the breakdown and destruction efficiency of pulses can be calculated with their field strength spectrum $V(j\omega)$ and the frequency range $[f_1, f_2]$ in which the EUT is coupling in a resonant behavior. This description is based on frequency limited norms [2] which are defined in Eq. 1.

With those norms it is possible to describe the threat parameters of a given wide band pulse. The most interesting efficiencies are the energy- and amplitude efficiency η_E and η_A which describe how much of the energy and the amplitude of a given pulse is coupling into the EUT.

$$\eta_E = \frac{\|V(j\omega)\|_{f,2}^{(f_1,f_2)}}{\|V(j\omega)\|_{f,2}}; \quad \eta_A = \frac{\|V(j\omega)\|_{f,1}^{(f_1,f_2)}}{\|V(j\omega)\|_{f,\infty}} \quad (2)$$

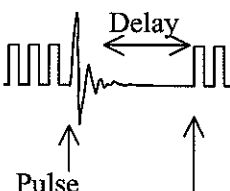
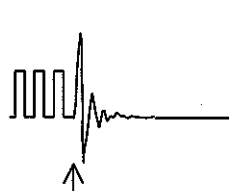
Breakdown	Destruction
 <p style="text-align: center;">Pulse</p> <p style="text-align: center;">Self-, External-, Power-Reset</p>	 <p style="text-align: center;">Puls</p>
Breakdown Failure Rate	Destruction Failure Rate
$BFR = \frac{\text{No. of Breakdowns}}{\text{No. of Pulses}}$	$DFR = \frac{\text{No. of Destructions}}{\text{No. of Pulses}}$

Fig. 1: Definition of the Breakdown Failure Rate and Destruction Failure Rate

To calculate the real threat potential of a given pulse to a EUT, described by his resonant coupling range $[f_1, f_2]$, one has to evaluate the average spectral amplitude

$$\rho_A = \|V(j\omega)\|_1^{f_1, f_2}; \rho_E = \|V(j\omega)\|_2^{f_1, f_2} \quad (3)$$

ρ_A and ρ_E energy density:

IV. GENERAL MEASUREMENT SETUP

All susceptibility data was taken by applying an electro-magnetic field to the EUT in a TEM structure. Exemplary we will describe the two mostly used TEM waveguides (see Figure 2) and the setup of the different EUT. The open area waveguide is a NEMP test simulator with a maximum height of about 23 m described in [3]. The laboratory waveguide [4] is an open waveguide inside a shielded room enclosed by absorber walls. The absorbers at the end of the waveguide were placed on interchangeable wooden walls. The position of the septum can be adjusted via nylon threads. The measurements of the electromagnetic properties were done by a Time Domain Reflectometer (TDR) as well as electric and magnetic ground plane and free field probes.

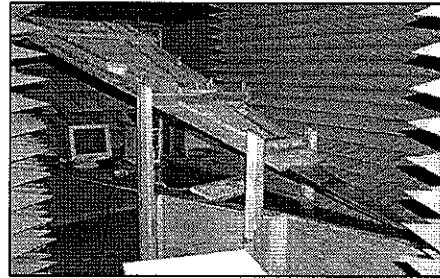
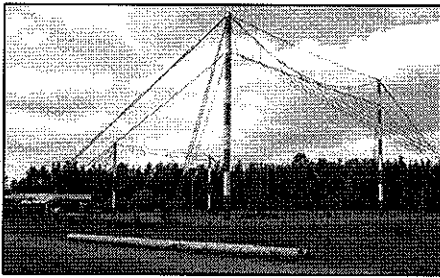


Fig. 2: Open Area TEM waveguide and

Laboratory TEM waveguide at the WIS, Munster

The different EUT were placed in the TEM structure as shown in Figure 3. During the test procedure different EUT signals as well as the field pulse were monitored with a real time scope (bandwidth: 6 GHz, sampling rate: 20 GSample).

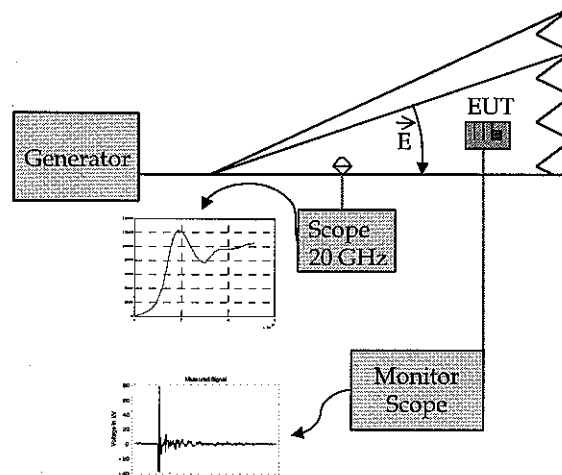


Fig. 3: General Measurement Setup

V. MEASUREMENT RESULTS

In this chapter a short extract of the most interesting results of the susceptibility investigations is given. Different electronic devices like logic elements, microcontrollers, PC-Systems and PC-Networks were tested.

A. Logic Devices

During the investigations ten different semiconductor technologies (six TTL-, four CMOS-families) have been tested (see Table II) concerning the susceptibility to EMP and UWB pulses. NANDs, inverter, generic array logic devices and shift registers were chosen to observe the influence of the technology on the destruction effects.

TABLE II
TESTED TECHNOLOGIES

TTL-Technology					
Standard	Schottky (S)	Low Power Schottky (LS)	Advanced Schottky (AS)	Advanced Low Power Schottky (ALS)	Fairchild Advanced Schottky (FAST)
CMOS-Technology					
High Speed (HC)	High Speed TTL-compatibel (HCT)	Advanced (AC)	Advanced TTL-compatibel (ACT)		

To apply the different pulses to the EUT a modular setup has been realized (Figure 4). Ten separate channels were built with a combination of differently printed circuit boards. The circuit boards were combined with ribbon cables to realize different coupling lengths at the input and output pins of the devices under test.

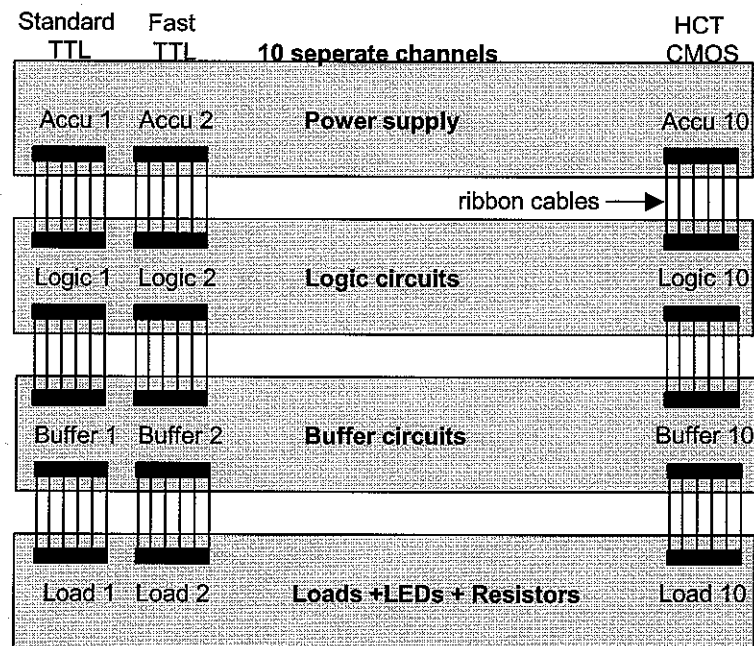


Fig. 4: Test setup

The power supply was made with ten different accumulators. DIP switches were implemented in the power supply unit to adjust arbitrary bit patterns at the input pins. LEDs and resistors were used as loads to observe the operating states of the devices. As a first result it can be noticed, that CMOS-devices first are affected by reversible breakdowns which can be fixed by switching the power off and on. At much higher field amplitudes destructions occur. This effect can be explained by a parasitic thyristor (latch up effect) as a result of the vicinity of complementary n- and p-channel transistors in CMOS devices described in [5].

Figure 5 shows the *BFR* and *DFR* of NAND-devices built in four different CMOS technologies. The comparison of CMOS- with TTL-NAND-device shows, that the destruction thresholds are similar, but that TTL-NAND-devices only show non reversible destructions. At lower field amplitudes no breakdowns occurred in the TTL NAND devices in contrary to the behavior of CMOS-NAND-devices (see Figure 6).

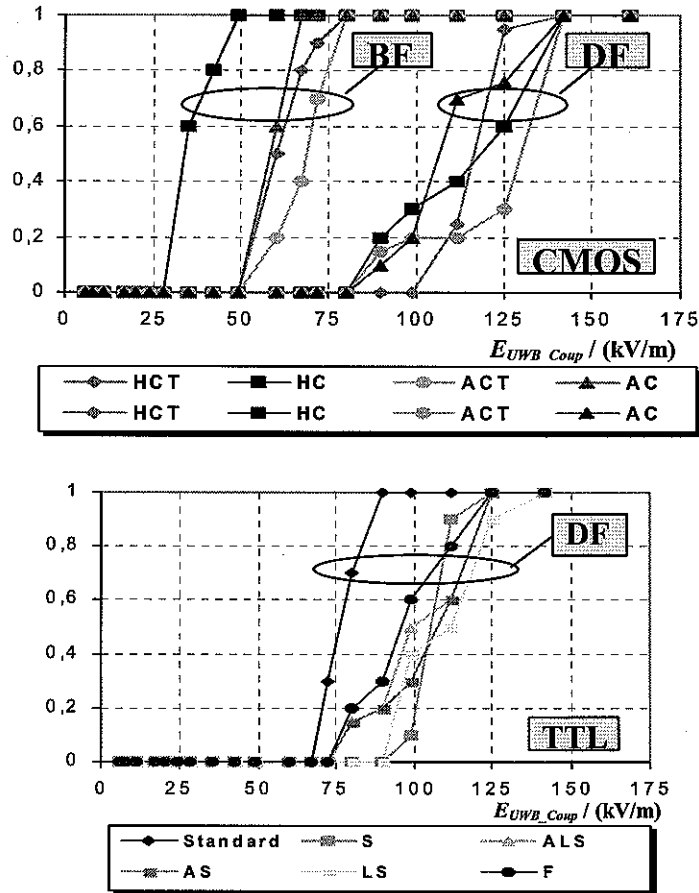


Fig. 6: Destruction Failure Rate (DFR) of TTL NAND Devices

Figure 7 shows the Breakdown- (*BT*) and Destruction threshold (*DT*) of NAND-devices built in ten different technologies (compare Table II). The same effects were observed during the investigation of inverter devices (Figure 8).

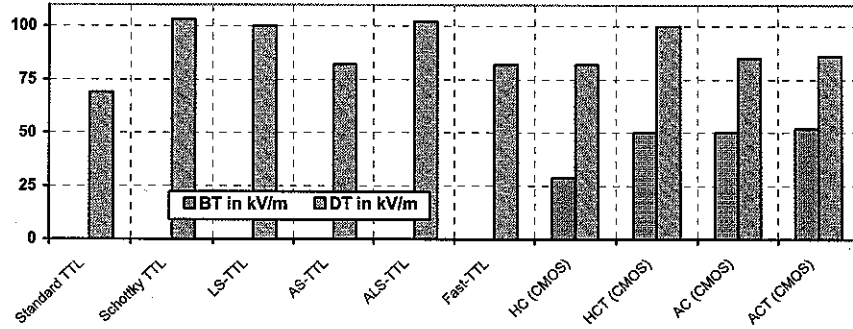


Fig. 7: Breakdown (BT) and Destruction (DT) Threshold of CMOS and TTL NAND Devices

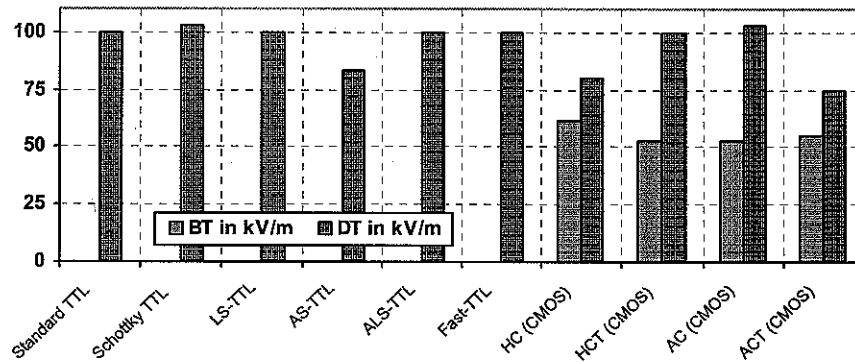


Fig. 8: Breakdown (BT) and Destruction (DT) Threshold of CMOS and TTL Inverter Devices

B. Microcontroller

Three different types of microcontrollers with a different number of I/O-ports have been investigated. The basic features of the microcontrollers are:

- RISC Architecture
- High-speed CMOS Technology
- 32 x 8 General Purpose Working Registers
- Flash on Board
- EEPROM on Board
- Power supply V_{CC}

The influence of different data-, reset-, oscillator.- and power supply-line lengths has been tested as well as a variation of the clock rate.

Figure 9 shows the basic elements of a micro controller circuit and the modified parameters. Four micro controllers of the same type have been tested simultaneously to observe any difference. The micro controller circuits were placed

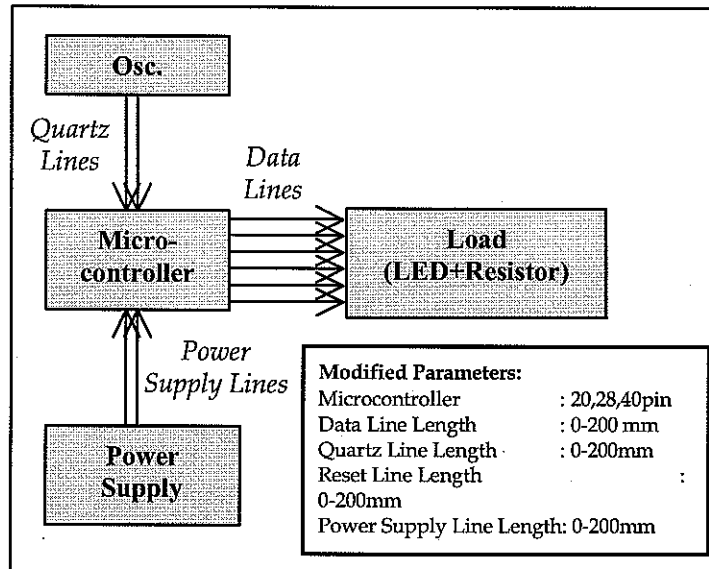


Fig. 9: Basic microcontroller circuit and modified parameters

vertically on a wooden wall (see Figure 10). The different states of the I/O-ports are monitored via different colored LED's.

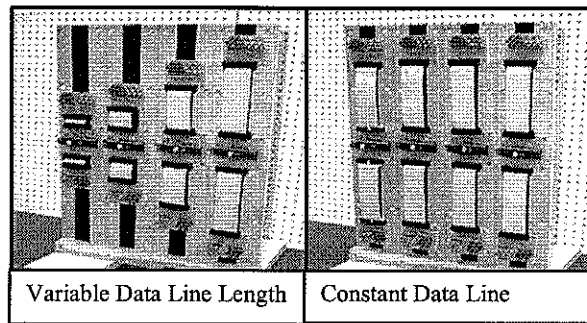


Fig. 10: Microcontroller test setup

The variation of the data-, osc.-, reset- and power supply-line length was done with ribbon cables.

During the test a program was running on the micro controllers which can get into two different states. In status 1 two ports are high and two ports are low to observe this state. After a switch the program moves to the second state in which the micro controllers were exposed to the pulses. The intention was to observe a self reset of the system by changing from state 2 back to state 1. Without the implementation of two states a self reset cannot be observed due to the fast reset action. In state 2 the I/O-Ports are changing from low to high to investigate the influence of the port state on the susceptibility.

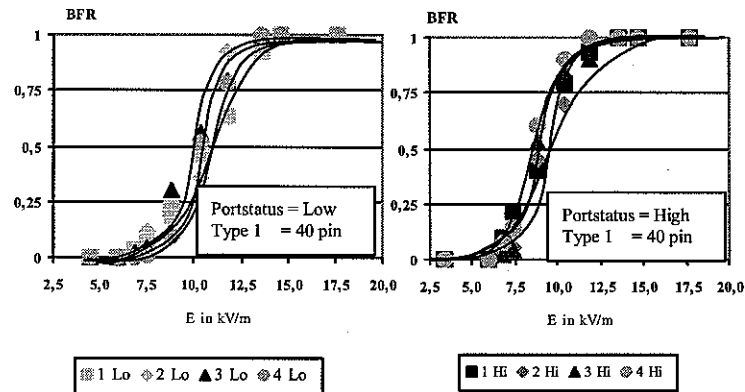


Fig. 11: Breakdown Failure Rate for micro-controller type 1 (40 pin) at basic setup

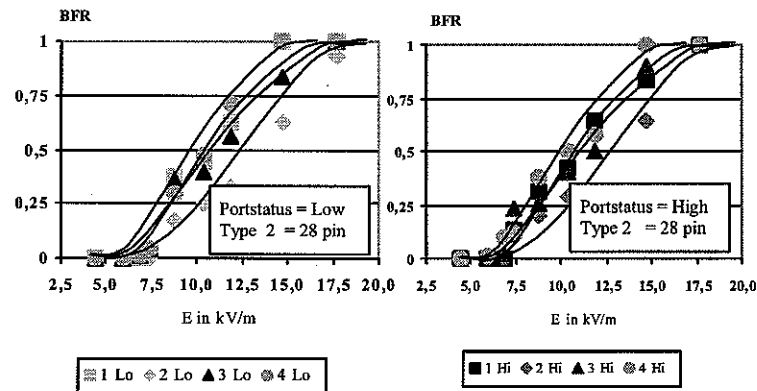


Fig. 12: Breakdown Failure Rate for micro-controller type 2 (28 pin) in a basic configuration

As the basic configuration a state with a minimal quartz-, reset-, data- and power supply lines length and a clock rate of 1 MHz was defined. Figures 11 and 12 show the results for two different types of microcontrollers in the basic configuration. For the microcontroller circuits *BT* and *BB* do not vary significantly when different devices of the same type of microcontroller were tested as shown in Figure 11 and 12, but are significantly influenced by the microcontroller type. In the analysis the breakdown parameters *BT* and *BB* have been determined as the average over the *BT* and *BB* of four microcontrollers of the same type.

TABLE III
INFLUENCE ON *BT* AND *BB*

	Data Line Length	Reset Line Length	Quartz Line Length	Power Supply Line Length	Clock Rate	Type of Controller
BT	Low	High	Medium	Medium	None	Low
BB	None	High	Low	Medium	None	High

The *BT* of the tested microcontrollers was generally significantly influenced by the reset line length, influenced by the clock- and power supply line length, not much influenced by the data line length and the type of microcontroller and not influenced by the clock rate (up to 8 MHz). These results are shown in Table III.

The *BB* is generally significantly influenced by the type of microcontroller and the reset line length, influenced by the power supply line length, not much influenced by the quartz line length and not influenced by the data line length and clock rate.

C. Microprocessor Boards

In this section the results of the determination of the susceptibility levels of microprocessor boards (MB) in several different test facilities are presented. Examined were two different MB:

1. SSC 5x86 AMD 133 MHz
2. Rocky-518HV Pentium/MMX 233 MHz

In Table IV the important parameters of the applied pulses are listed. To compress the large number of results of all those tests to a manageable number, for HPM and cw signals the highest (HL) medium (ML) and smallest (SL) susceptibility level over the frequency was determined. The HL (ML) is the highest (average) field strength needed to disrupt the EUT over all tested frequencies. Accordingly SL is the smallest field strength needed to disrupt the EUT over all tested frequencies, what means that the frequency of the SL is the most susceptible frequency of the EUT.

TABLE IV
PARAMETERS OF THE TEST PULSES

Pulse Shape	Parameter 1	Parameter 2	Parameter 3
EMP 10	t_r 10 ns	t_{whm} 200 ns	E_{max} up to 50 kV/m
EMP 1	1 ns	80 ns	up to 50 kV/m
WIS UWB up	t_r 90 ps	t_{whm} 2.5 ns	E_{max} up to 30 kV/m
WIS UWB bp	t_r/t_f 100 ps	t_d 350 ps	E_{max} up to 20 kV/m
Rheinmetall UWB bp	200 ps	500 ps	up to 40 kV/m
HPM	<i>Freq.-Range</i> 150 MHz –	<i>PRF</i> 1 Hz –	E_{max} up to 4 kV/m
dwell time 1 s	3.4 GHz	1 kHz	
cw	80 MHz – 1000 MHz	dwell time 1 s	up to 1 kV/m

For pulsed signals another quantity is of importance: the breakdown bandwidth (BB). The lower border of the BB represents a low probability of disruption by a single pulse, so a high PRF (HPRF) is needed to disrupt the MB, the upper border represents a high probability for a disruption by a single pulse, so only a low PRF (LPRF) is needed to disrupt the MB. The compressed results of the susceptibility levels of the MB are shown in figure 13 for EMP and UWB pulses and in Figure 14 for HPM and cw signals. The susceptibility of the 133 MHz MB is comparable to the shown results.

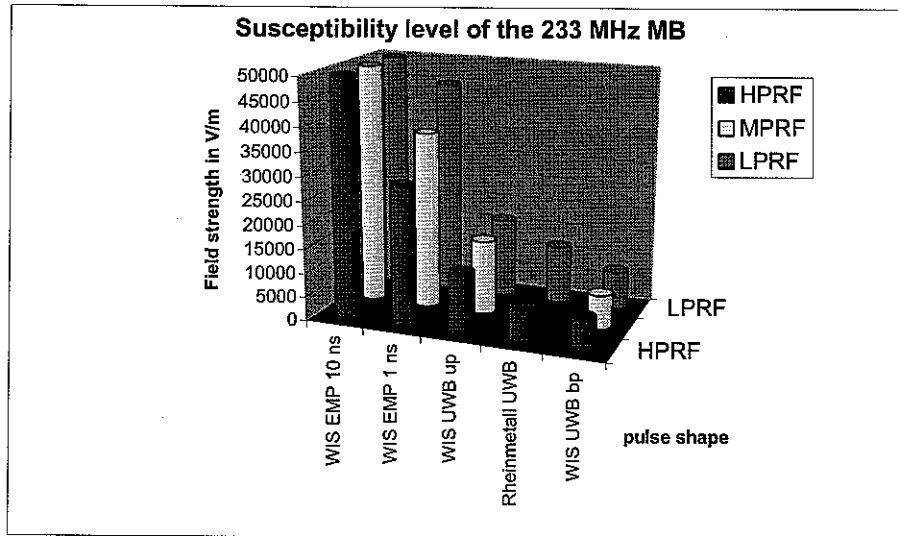


Fig. 13: Susceptibility levels of the 233 MHz MB to EMP and UWB

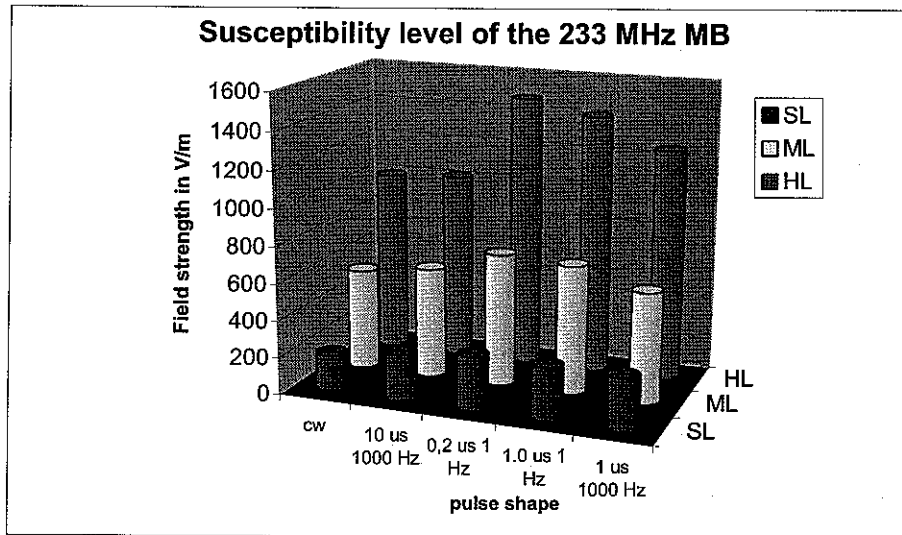


Fig. 14: Susceptibility levels of the 233 MHz MB to HPM and cw signals

A first look at those susceptibility levels leads to the following results:

The difference between the susceptibility levels of long HPM pulses and cw signals is small. The duration of HPM pulses (above a certain minimal duration) has nearly no influence on the susceptibility levels of the MB. The effect of the repetition rate of the HPM pulses on the susceptibility levels of the MB is only of minor significance. The SL value for both MB is about a few 100 V/m, the HL value of both MB is located between 1 kV/m and 2 kV/m. The effect of a rising of the PRF for EMP and UWB pulses is significantly lowering the susceptibility levels. The susceptibility levels are extremely dependent on the pulse shape (in the case of the used pulse shapes the maximal difference of the susceptibility levels was a factor of 25 in necessary field strength). The lowest susceptibility levels for EMP and UWB pulses are a few kV/m.

For a more detailed evaluation of the results with regard to the susceptibility levels and the pulse characteristics one has to take some more complex time- and frequency domain quantities into account which have to be determined and discussed. In the following quantities which were selected for the detailed evaluation

are introduced. In the time domain the maximal amplitude $\hat{A}(t)$ (HL and SL for HPM and cw signals and HPRF and LPRF for EMP and UWB pulses), the overall energy density of the field signal $\hat{E}(t)$, the PRF efficiency and the frequency efficiency

$$\eta_{PRF} = \frac{E_{HPRF}}{E_{LPRF}} \text{ and } \eta_{Freq} = \frac{E_{SL}}{E_{HL}}$$

were selected. In the frequency domain the maximal spectral amplitude $\hat{A}(f)$, the average spectral amplitude ρ_A and energy density ρ_E and the amplitude- and energy efficiency η_A and η_E were selected in the frequency range from 100 MHz to 3 GHz, because in that frequency range the coupling efficiency of the MB is optimal [6]. One of the most important quantities for the evaluation of HPM pulses is η_{Freq} because it is a measure for the effectiveness of a HPM pulse in the case that the system transfer function, the orientation of the system and the actual layout of the cable bundles of the target system are not known. The frequency efficiency of both MB for the different pulse shapes has an average of about 0.2 which leads to the assumption that the quality of the coupling resonances is very low (near 5). A similarly important quantity is η_{PRF} for EMP and UWB pulses because it determines whether it makes sense to use repetitive pulses for disrupting a given system or not. The PRF efficiency of the two MB for all used EMP and UWB pulse shapes has an average value of 0.7 what means that the usage of a repetitive system would lower the susceptibility level by approximately 30% compared to a single shot system. The energy density which is necessary for a disruption of the MB is of large importance for the selection of the source and the power supply and determines their weight and size. This energy density is shown in Figure 15 for two cases: best case (black): the SL value for HPM and cw signals and the HPRF level for EMP and UWB pulses) and worst case (gray) the HL value for HPM and cw signals and the LPRF level for EMP and UWB.

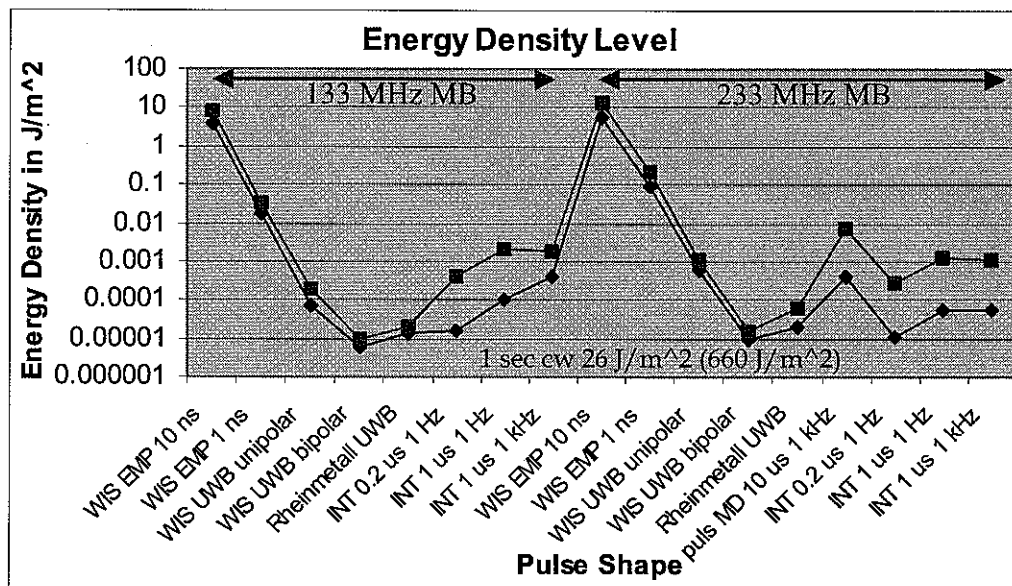


Fig. 15: Energy density of the pulses for both MB

Depending on the pulse shape some pulses need a million times the energy other pulses need for a disruption of the MB functionality. Noticeable is that the most effective HPM pulse in the best case scenario (SL) needs only 2 or 3 times the energy a UWB pulse needs to disrupt the MB. In the worst case scenario the most effective HPM pulse needs 60 to 70 times the energy of the UWB pulse.

The large differences in the susceptibility levels for different EMP and UWB pulses are demonstrating that an evaluation of the pulse efficiencies in the time domain is not sufficient. The determination of the energy- and amplitude efficiencies is making clear why those susceptibility levels differ that much. The pulses which do not have distributed their power and energy in the for MB relevant spectral range [2] have a very low energy- and amplitude efficiency which does analytically explain the measured values. Even the highest measured difference in the for a disruption necessary energy of the different pulses (10^6) and the maximal difference of the energy efficiency is the same (factor of 10^6 between EMP 10 and WIS UWB bp).

The average spectral amplitudes of the pulses determine the amount of coupled voltage or current in the system. The average spectral amplitude of 10^{-5} V/m/Hz at the for the disruption of the MB necessary field strengths is the same for all pulse shapes. A HPM signal needs between 2 and 71 times the energy a UWB pulse needs to disrupt the MB but only a factor of 0.03 to 0.45 of the field strength.

D. PC - Systems

During the investigation the tested PC systems were operated in a minimal configuration which consists of mainboard, processor, random access memory and accumulator power supply. For monitoring the function of the systems, an ISA-bus monitor card has been developed which allows to monitor data lines, address lines and internal system states separately. Those systems were placed in the waveguides in such, that coupling into the monitor card is minimal. A simple DOS version has been chosen as the operating system to avoid breakdowns as a result of a higher level operation system. The operation system as well as the test programs were loaded directly before the test from a floppy disk drive, so that no hard disk drive was necessary.

To observe the influence of different program states concerning the susceptibility of personal computers, a test program with separate subroutines has been implemented in the investigated PC systems. Different hardware elements (Direct Memory Access controller (DMA) and Programmable Interval Timer Module (PIT)) on the mainboards were activated. The DMA-main-routine as well as the PIT-main-routine is separated into three subroutines with different functions inside the DMA-controller resp. the PIT-module. During each subroutine, the pulses have been applied to the systems. After each subroutine a CPU test has been performed to make sure that the complete system was working properly. Fig.16 shows the breakdown thresholds BT of three personal computer systems for an UWB testpulse with a rise time of $t_r = 100$ ps and a pulse length of $t_{whm} = 2,5$ ns.

Neither in the main routines nor in the sub routines a significant change of the breakdown thresholds BT has been observed. The BT gets smaller the higher the generation of the technology is. Similar results have been observed if pulses with other rise times and pulse lengths were applied.

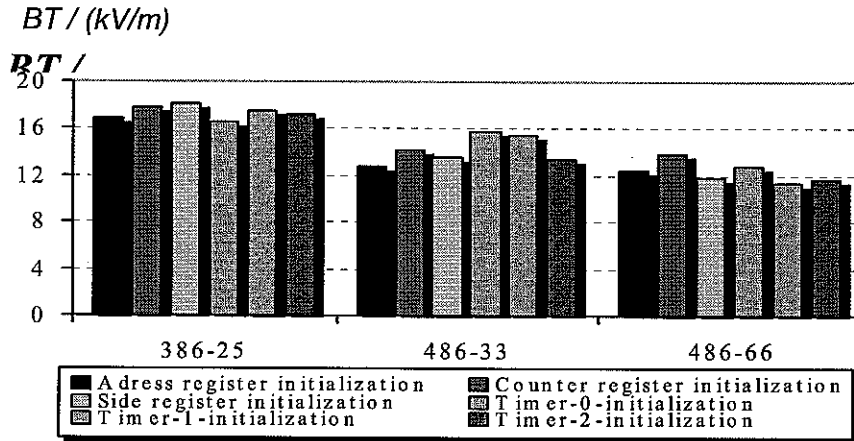


Fig. 16: Breakdown Threshold BT of three personal computer systems in six different

E. PC – Networks

The susceptibility levels of a PC – network consisting of two i486 based personal computers and an Ethernet connection to unipolar UWB pulses with a rise time of 100 ps, a full width half max time of 2.5 ns and an amplitude of 100 V/m to 12000 V/m was tested. Several network configurations and cables were used:

- 10Base2
- 10BaseT
- 100BaseTX
- Ethernet Hub
- RG 58, RG 223, S-UTP and S-STP cables
- 10 MBit and 100 MBit

To eliminate the susceptibility effects of the PCs we shielded the two PCs with movable absorber walls (see Figure 17)

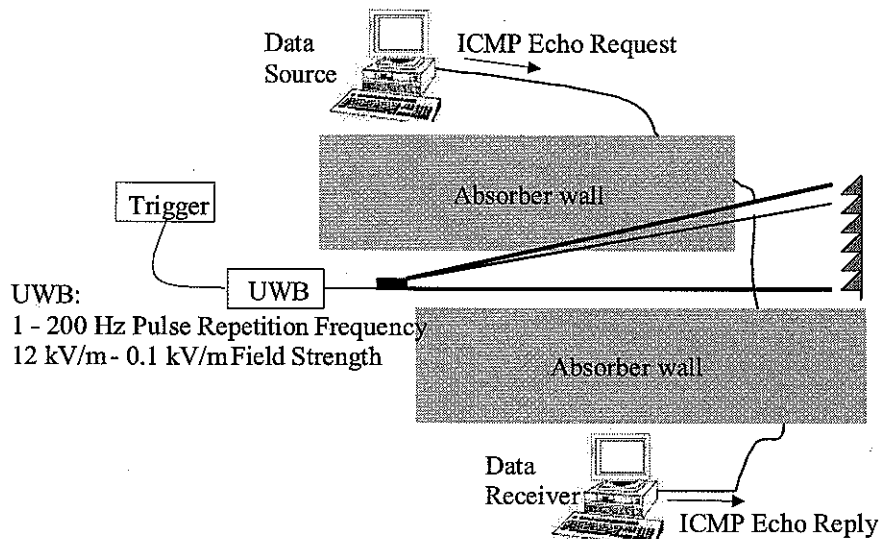


Fig. 17: Measurement setup for the PC – Network tests

The data line was exposed to the UWB pulses and the number of bit errors, lost data frames, and PC breakdowns was monitored. A collision between signal bits on the network and a coupled UWB pulse is shown in Figure 18. The coupled pulse

resulted from a 12 kV/m UWB pulse coupling into a RG 58 cable. The amplitude of the coupled pulse was 90 V.

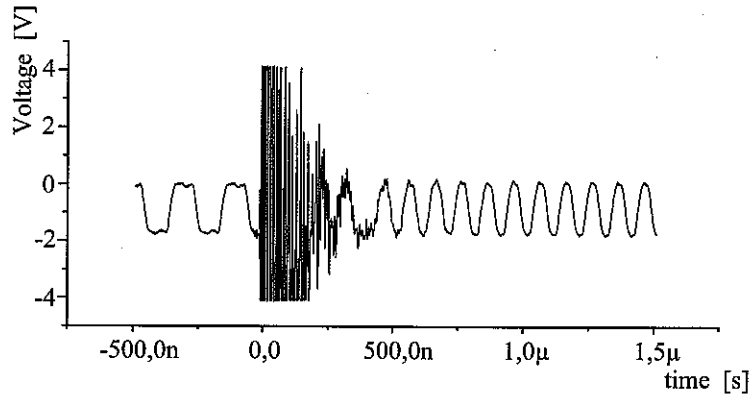


Fig. 18: Collision of a coupled UWB pulse with data bits

The UWB field strength level which lead to bit errors, lost frames or to a breakdown of the network are shown in Figure 19. Bit errors occur when the amplitude of the coupled pulse is comparable to the voltage level of the bits. Data frames are lost when a substantial part of the frame is destroyed by the coupled pulse. This quantity rises linearly with the pulse repetition frequency. A breakdown occurs when the coupled signal is so large, that the network hardware locks or resets.

The susceptibility depends strongly on the shielding effectiveness of the used cables and the technology used (see Figure 19). The lowest UWB field strength level for bit errors is 200 V/m, for lost frames about 4 kV/m and for breakdowns about 6 kV/m. [6]

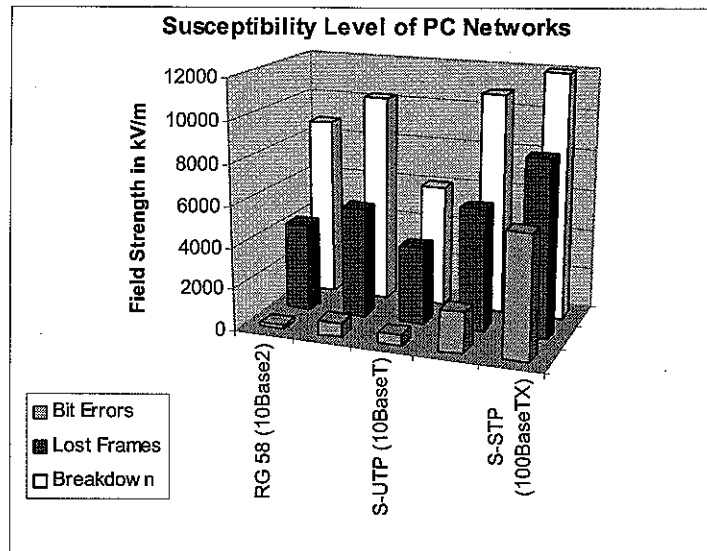


Fig. 19: Susceptibility level of PC Networks

F. Microscopic Analysis of Destruction Effects

The microscopic analysis of the destructed devices generally shows three different damaging levels (Figure 20). At lower field strengths (level 1) only electronic components like diodes or transistors on the chip were damaged, mostly as a result of flashover effects (Figure 20).

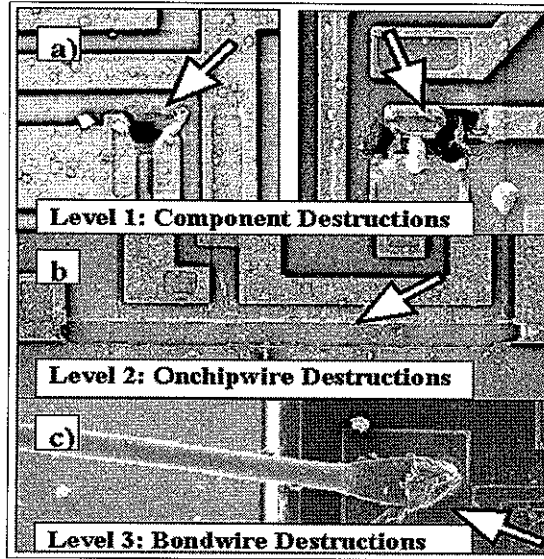


Fig. 20. Destruction effects on chip level

If the amplitude of the electromagnetic pulse increases by about 50 %, additional on chip wire destructions (this means smelting of pcb tracks without flashover effects) and multiple component destructions occurred (Figure 21, level 2). Further increase of the amplitude leads to additional bond wire destructions (Figure 21) and multiple component- and on chip wire-destructions (level 3).

Figure 21 shows the destruction failure rate (DFR) of TTL-Inverter devices, separated to component-, on chip wire- and bond wire-destruction. At the lowest field level component destructions occur. A further rising of the field strength resulted in on chip wire- and bond wire-destruction. The components on the chip, which were damaged first if the amplitude of the electromagnetic pulse was increased, are depending on the layout of the chip (and therefore on the manufacturer) as well as on the technology.

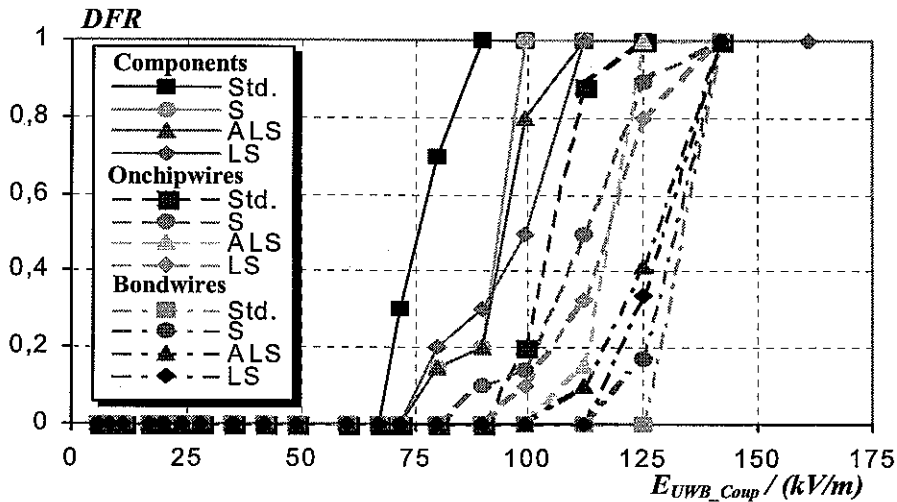


Fig. 21. DFR of TTL-NAND-Devices separated into Component- Bond wire- and On chip wire- Destructions

Transistors, diodes and resistors were damaged similarly. The reproducibility of the destruction effects on chip level in the used measurement setup is very high. On that

account it is possible to predict the destruction effects of integrated circuits on chip level, if the proposed measurement setup is used.

VI. CONCLUSION

The main goal of this paper was to give a brief overview of the susceptibility levels of modern electronic equipment as well as the breakdown and destruction effects. In Table V the susceptibility levels (lowest observed field strength for a disruption of the functionality of the EUT) of all tested devices are shown. Generally the level is the lower the more complex the device under test is. The investigation of the destruction effects show, that even UWB pulses have sufficient energy to destroy on chip structures.

TABLE V
SUSCEPTIBILITY LEVELS BT (DT)

EUT	UWB in kV/m	EMP in kV/m	HPM in kV/m
Logic Devices	25 (75)	120	
Microcontroller	7.5	42	
Microprocessor Boards	4	25	0.2
PC Systems	12		
PC Networks	0.2	0.5	

References:

- [1] D. Nitsch, F. Sabath, C. Mojert, M. Camp, J.L. ter Haseborg, "Susceptibility of electronic equipment to transient electromagnetic fields of various waveforms", International Conference on Electromagnetics in Advanced Applications, ICEAA, pages 213-216, Turino, Italy, September 2001
- [2] D. Nitsch, F. Sabath, „Prediction of Ultra Wide Band Coupling to modern Electronic Equipment“; Proceedings of the EMC Wroclaw, Wroclaw, Poland, June 2002, pp. 103 – 108
- [3] D.Nitsch, J.Schlüter, H.J.Kitschke,, "Generierung und Vorteile von Ultrawideband-Impulsen", EMV99, Mannheim, Germany
- [4] C.Braun, "Aufbau eines breitbandigen Wellenleiters für NEMP Modell Simulationen", INT Bericht Okt. 84
- [5] Haselhoff, E.: „Latchup, ESD, and Other Phenomena“, Texas Instruments, 2000
- [6] C. Mojert, D. Nitsch, H. Friedhoff, J. Maack, M. Camp, "UWB and EMP Susceptibility of modern Computer Networks", EMC Zürich 2001, Zurich (Switzerland), February 2001